

# Sleep apnea-hypopnea quantification by cardiovascular data analysis

Sabrina Camargo<sup>1,2,3\*</sup>, Maik Riedl<sup>1</sup>, Celia Anteneodo<sup>3,4</sup>, Jürgen Kurths<sup>1,5,6</sup>, Thomas Penzel<sup>7</sup>, Niels Wessel<sup>1</sup>

**1 Department of Physics, Humboldt-Universität zu Berlin, Berlin, Germany**

**2 EMap, Fundação Getúlio Vargas, Rio de Janeiro, Brazil**

**3 Department of Physics, PUC-Rio, Rio de Janeiro, Brazil**

**4 National Institute of Science and Technology for Complex Systems, Rio de Janeiro, Brazil**

**5 Potsdam Institute for Climate Impact Research, Potsdam, Germany**

**6 Institute for Complex Systems and Mathematical Biology, University of Aberdeen, Aberdeen, United Kingdom**

**7 Sleep Center, Charité University Hospital, Berlin, Germany**

\* E-mail: [sabrina.camargo@fgv.br](mailto:sabrina.camargo@fgv.br)

## Abstract

Sleep apnea is the most common sleep disturbance and it is an important risk factor for cardiovascular disorders. Its detection relies on a polysomnography, a combination of diverse exams. In order to detect changes due to sleep disturbances such as sleep apnea occurrences, without the need of combined recordings, we mainly analyze systolic blood pressure signals (maximal blood pressure value of each beat to beat interval). Nonstationarities in the data are uncovered by a segmentation procedure, which provides local quantities that are correlated to apnea-hypopnea events. Those quantities are the average length and average variance of stationary patches. By comparing them to an apnea score previously obtained by polysomnographic exams, we propose an apnea quantifier based on blood pressure signal. This furnishes an alternative procedure for the detection of apnea based on a single time series, with an accuracy of 82%.

## Introduction

Sleep disturbances (e.g., sleep apnea, insomnia, restless legs syndrome, sleep walking, sleep terror) deserve serious attention since they constitute an important risk factor for cardiovascular disorders such as hypertension, cardiac ischemia, sudden cardiac death, and stroke [1–3]. Cardiorespiratory data, such as heart rate variability and respiratory variability, can be useful to detect the sleep disturbances, especially the most common sleep apnea. Individuals suffering this kind of disorder usually present daytime sleepiness, loud snoring and restless sleep. A sleep apnea event is defined as a pause of the airflow lasting at least 10 secs. If the air flow is lower than 50% of normal, the resulting airflow limitation is called a hypopnea [4]. When there is no inspiratory effort, then the event is classified as central. If respiratory effort is made against an upper airway obstruction, then the apnea event is classified as obstructive. Sleep apnea events can be also of a mixed type.

In order to obtain a sleep profile the common practice is to combine records collected by means of different exams: electroencephalography (EEG), electromyography (EMG), and electro-oculography (EOG). This set produces a polysomnography, from which a visual scoring of sleep stages is evaluated, assigning to each stage the pattern found in consecutive 30-second-long epochs of the EEG, EMG, and EOG recordings. The resulting succession of discrete sleep stages is referred to as hypnogram and supports diagnostic decisions [5].

Signals of airflow, respiratory effort such as abdominal movement and oxygen saturation of the blood are used in diagnosis of sleep apnea [6], and as mentioned before, it requires combined records. Therefore, it would be desirable to evaluate sleeping through an alternative procedure consisting of simpler data recordings. This is the goal we pursued in the present work.

It is important to emphasize that cardiorespiratory time series are highly nonstationary, what restricts the use of standard tools. In that regard, Penzel et al. showed that changes in heart rate variability in obstructive apneas were better quantified by scaling analysis (using detrended fluctuation analysis) than by spectral analysis [7, 8]. This is because, techniques such as fast fourier transformation require stationarity in order to obtain a meaningful

estimation of the spectral components that are found in a time series [9]. Hence, to deal with nonstationarity of heart rate variability, as well as of blood pressure variability, and consequently allowing the application of techniques like spectral analysis, we apply a nonparametric segmentation procedure to yield patches where stationarity is verified. In such locally stationary segments, the statistical measures mean and variance remain constant. Segmentation provides an indication of nonstationarity of a time series, in particular, the intrinsic time scales. Moreover, by finding the stationary regimes, one might be able to identify changes in time series, as those coming from the apnea occurrence.

## Materials and Methods

The study and the consent procedure were approved by the ethics committee, Charité - Universitätsmedizin, in Berlin. Participants provided their written informed consent to participate in this study and the informed consent of all subjects was recorded in paper form. We analyzed data from 26 patients suffering from apnea-hypopnea, that is with apnea-hypopnea index (AHI, the average number of apnea events per hour) larger than 15, considering obstructive, central, and mixed sleep apnea events. The patients were then divided into two groups, according to their diurnal systolic blood pressure levels: 10 hypertensive subjects (HT) and 16 normotensive patients (NT). The mean values of the systolic blood pressure were  $142 \pm 4/93 \pm 8$  mmHg in HT and  $120 \pm 10/81 \pm 7$  mmHg in NT. Moreover, we add a control group (C) with 7 non-apneic subjects. All three groups are age and sex matched, all male with mean age of  $44.1 \pm 8.1$  years (HT),  $44.6 \pm 7.6$  (NT), and  $44.8 \pm 6.7$  (C). The apnea-hypopnea indexes in the groups are  $1.0 \pm 1.6$  (C),  $42.5 \pm 24.0$  (NT) and  $71.7 \pm 32.7$  (HT).

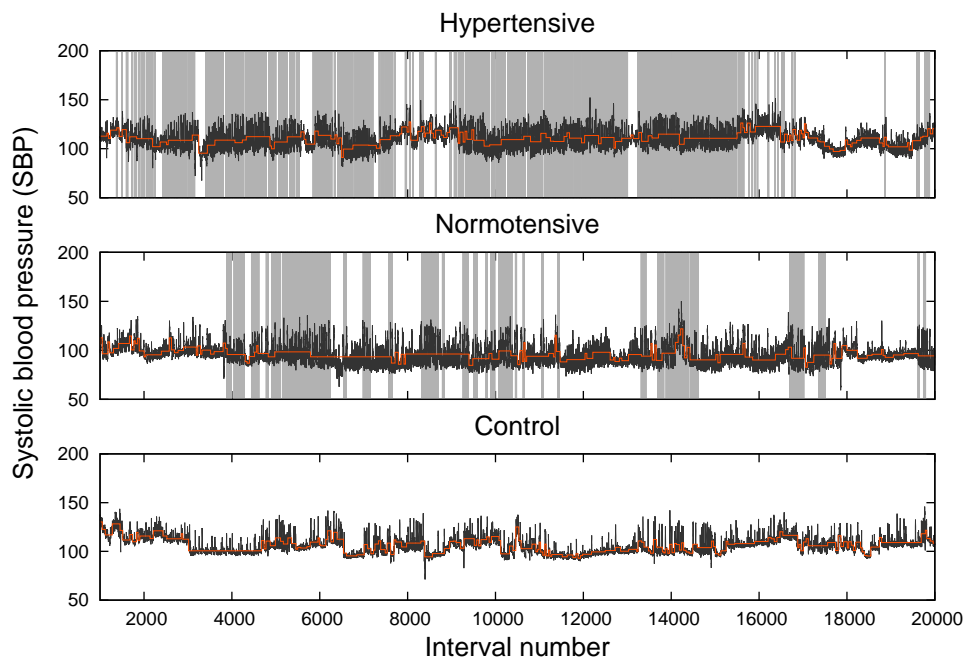


**Figure 1.** Systolic blood pressure (SBP) time series (black line) and its local mean values from segmentation (light orange line) for typical hypertensive (upper panel), normotensive (middle panel) and control (lower panel) subjects. Apnea events, detected via a polysomnography examination, are represented by the light gray vertical lines.

The intervals between successive heartbeats (beat-to-beat intervals) were extracted from 24h-electrocardiogram records [10]. To remove artifacts caused by, e.g., premature beats, the beat-to-beat intervals were filtered by means of interpolation using an adaptive filter [11]. Blood pressure was ‘continuously’ monitored (at a sampling rate of 200 Hz) with a finger cuff sensor (Portapres Model2, BMI-TNO). From the continuous blood pressure signal, the maximum value in each beat-to-beat interval was extracted, producing the time series of systolic blood pressure (SBP) on a beat-to-beat basis. Analogous procedure was followed by using minimum blood pressure values to extract the beat-to-beat diastolic blood pressure (DBP) [12–14]. Beat-to-beat intervals from blood pressure (BBI-BP) records and from electrocardiograms (BBI-EKG) were also analyzed. Results for SBP and DBP series are similar, but SBP presents slightly better evaluation. We will concentrate on SBP in the further description.

We first dealt with the nonstationarity of the series performing a segmentation into stationary-like patches based on the Kolmogorov-Smirnov (KS) statistics, which provides a set of stationary data segments that compose the signal [15]. The KS-segmentation procedure is done through the following steps: given the time series, all points of the signal are considered as a potential cutting point, and we compute the Kolmogorov-Smirnov distance  $D \equiv D_{KS}(1/n_L + 1/n_R)^{-1/2}$ , between the cumulative distributions of the points belonging to the two segments placed at the left and the right sides of the cutting point, with lengths  $n_L$  and  $n_R$ , respectively. Thus, there will be one value of  $D$  corresponding to a hypothetical cut at each point of the signal, and we determine the position  $i_{max}$  where  $D$  is maximal. Once we know the position  $i_{max}$  of the maximal distance  $D$ ,  $D^{max}$ , the statistical significance of this cut (at a desired significance level  $\alpha = 1 - P_0$ ) is verified by comparing  $D^{max}$  with the result that would be obtained by chance, given by the empirical curve  $D_{crit}^{max}(n) = a(\ln n - b)^c$ , and  $(a, b, c) = (1.52, 1.80, 0.14)$  for  $P_0 = 0.95$ , with  $n = n_R + n_L$ . The signal is then split into two segments if  $D^{max}$  exceeds its critical value for the selected significance level  $D_{crit}^{max}(n)$ . The procedure is then applied to each one of the segments, starting from the full series  $\{x_i, 1 \leq i \leq N\}$ , where  $N$  is the total number of data points, until no segmentable patches are left. (See Refs. [15, 16] for further details). We performed the KS-segmentation with  $\ell_0 = 30$ , the minimal segment length, and  $P_0 = 0.95$ . The choice of  $\ell_0 = 30$  is based on its correspondence to the higher edge frequency of the very low frequency band of the heart rate with 0.03 Hz [17].

Fig. 1 shows the time series of SBP (black lines) for typical members of hypertensive (upper panel), normotensive (middle panel), and control (lower panel) groups, with the first and second patients suffering from sleep apnea-hypopnea. The mean value of the data segments provided by the KS-segmentation procedure is also represented (light orange lines) to allow the reader to identify the stationary patches. For comparison, the sleep apnea events, detected via a polysomnography examination, are represented by the light gray vertical lines.

## Results

Let us analyze the segmentation portraits of the SBP time series. Concerning the duration of stationary patches, we show in Fig. 2 the complementary cumulative distribution of segment lengths. No substantial differences are found between the distributions of the two apneic groups. In contrast, they differ from the control group distribution, where larger patches are less frequent.

In order to inspect a possible correspondence between the typical duration of stationary segments and degree of apnea, we plot in Fig. 3 the mean segment length  $\langle L \rangle$  vs AHI, for each patient. As a matter of fact, a positive correlation between  $\langle L \rangle$  and AHI comes out (quantitatively, the Pearson coefficient is  $r = 0.77$ ). Moreover, one can set a threshold allowing to separate most apneic individuals. The threshold was chosen by minimizing the fractions of false negative and false positive results by means of ROC (receive operating characteristic) analysis [18]. This threshold allows to identify above 80% of apneic subjects. However, we will investigate if there are other quantities that might provide a better separation.

Let us now investigate the statistics of stationary segments. Since there is a tendency that apneic patients typically have larger mean variance (computed over all segments of each time series), then a natural candidate for separation is, in principle, the variability in each segment. In Fig. 4, we depict the local variance  $\sigma^2$  (variance of each patch) for one individual of each group. Notice that apnea epochs have a strong influence on the variability of the SBP signal, with increased dispersion (higher variance) in the gray areas, when compared to the scored apnea,

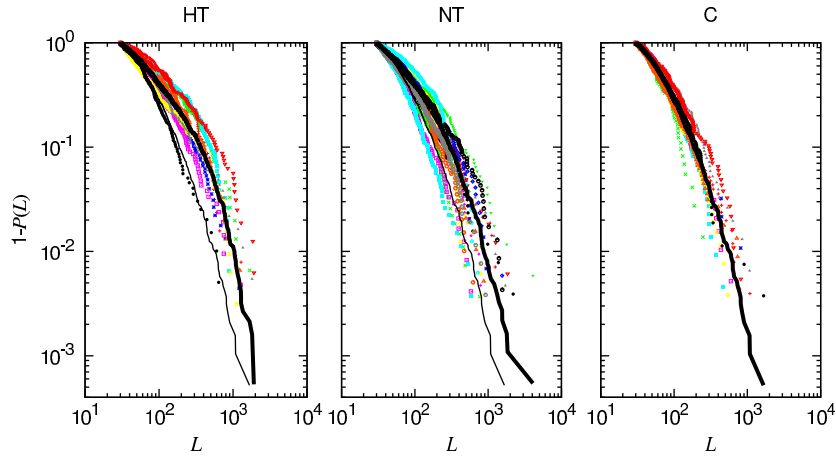


**Figure 2.** Complementary cumulative distribution of segment lengths for each individual (color) and accumulated data of all subjects in the same group (black solid line), for the hypertensive (HT), normotensive (NT) and control (C) groups. Drawn for comparison, the thin line in the first two panels (HT and NT) reproduces the control group accumulated data curve (C).

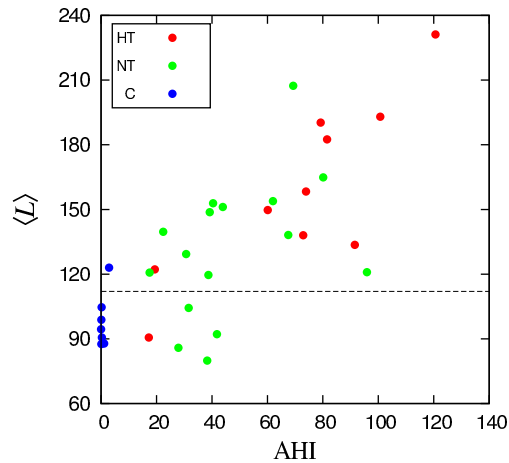


**Figure 3.** Mean length of the segments  $\langle L \rangle$  versus AHI for each subject. The dashed horizontal line represents the threshold value obtained by a ROC analysis.

both for the hypertensive and normotensive cases.

Taking into account all the individuals of each group, we computed the quartiles (the three points that define the four equiprobable intervals), for the average local variance  $\langle \sigma^2 \rangle$ , as shown in Fig. 5. Although there is a tendency that the control group presents lower dispersion, due to overlapping, no clear group separation occurs by considering only the average variance for each patient. This is reinforced by the observation of a relatively weak correlation between the mean variance and AHI, as exhibited in Fig. 6 (with  $r = 0.62$ ).

The average local mean  $\langle \mu \rangle$  is less efficient (with stronger overlap) than the average variance for separability purposes. The same arises when considering higher order moments, for which no significant differences amongst groups were detected.

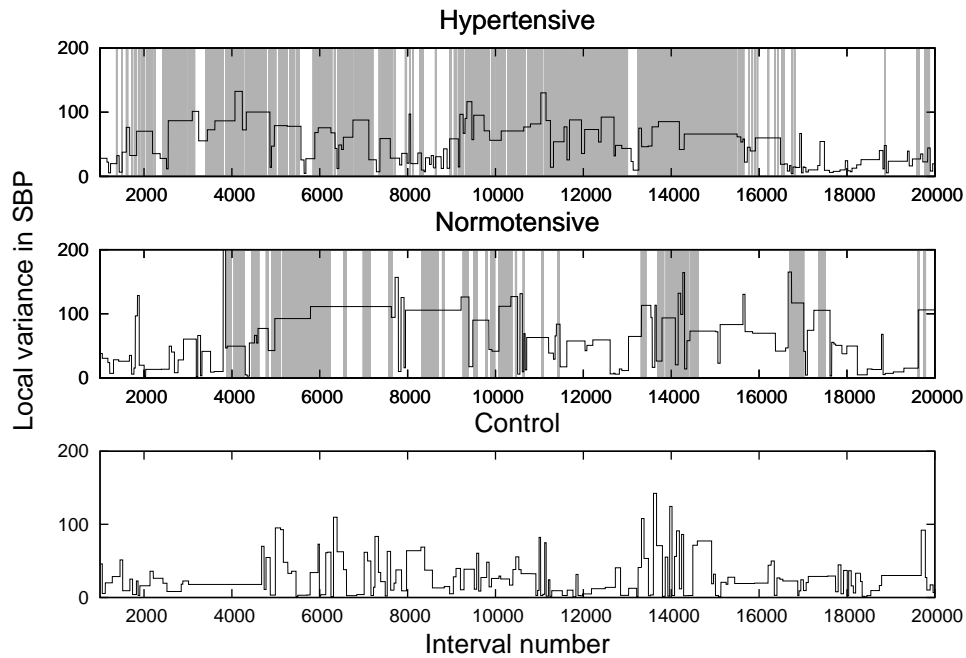


**Figure 4.** Local variance (black lines) provided by the segmentation of SBP and the standard apnea detection represented by the light gray lines, for the same examples of Fig. 1.

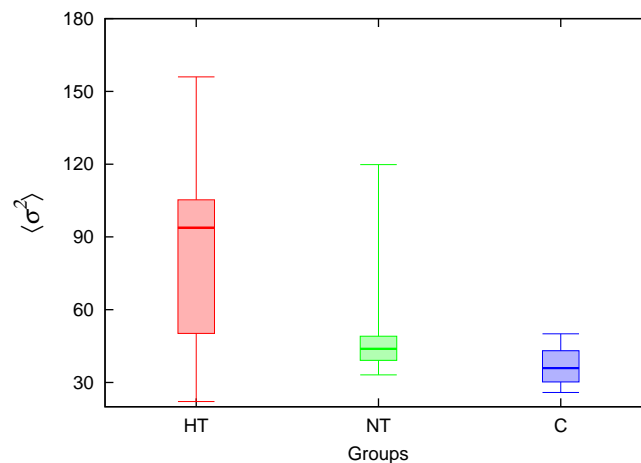


**Figure 5.** Quartiles of the distribution of the average variance  $\langle \sigma^2 \rangle$ , within each group. The horizontal lines limit the quartiles, the thicker one indicating the median.

The same analysis for the beat-to-beat series, BBI-BP and BBI-EKG, displayed weak correlations between the average length  $\langle L \rangle$  and AHI, with Pearson coefficient  $r = 0.11$  and  $0.05$ , respectively. Also a weak correlation between the mean variance  $\langle \sigma^2 \rangle$  and AHI was observed, with  $r = 0.05$  and  $0.03$ , respectively. Then, in further analyses, we concentrated on SBP, as a potential candidate for sleep apnea diagnosis.

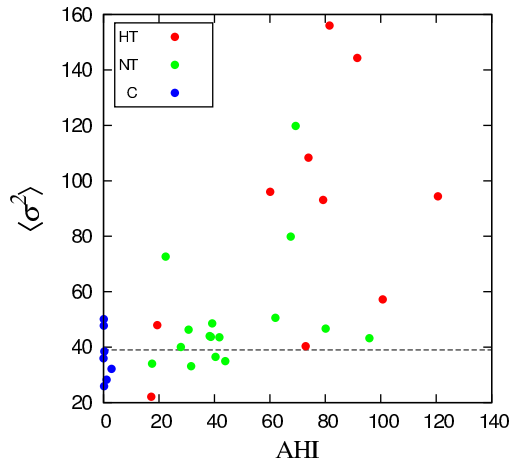


**Figure 6.** Mean variance of the segments  $\langle \sigma^2 \rangle$  versus AHI for each subject. The dashed horizontal line represents the ROC threshold.

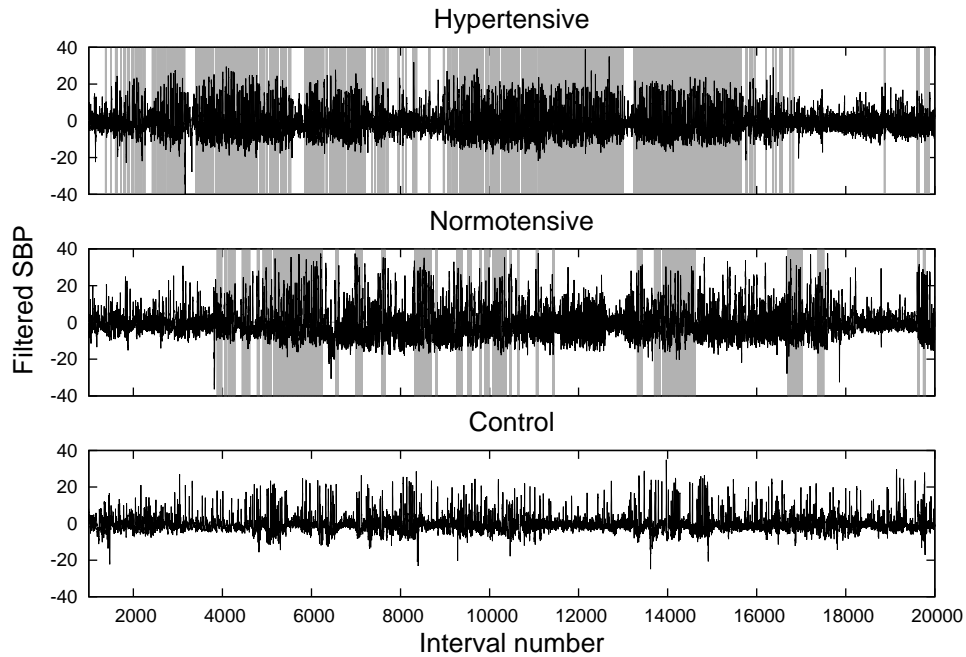


**Figure 7.** Systolic blood pressure time series, once the local mean,  $\mu$ , was subtracted (black lines) and standard apnea detection (light gray vertical lines).

The next step is to look at autocorrelations. In order to obtain a signal that can be analyzed through standard spectral methods, we subtract the local mean  $\mu$  (the mean value of each data segment) from the corresponding patch, yielding a filtered signal, as shown with black lines in Fig. 7. The removal of the local mean does not guarantee stationarity, as far as variance (e.g., Fig 7) and higher-order moments may still change. However, it

furnishes a detrended signal more stationary than the original one.

We then look at how the autocorrelation function of the filtered signal behaves for each individual of each group, as shown in Fig. 8. The autocorrelation function displays a noticeable behavior, with oscillatory patterns, which are more pronounced in subjects with sleep apnea, while rapidly vanishing for the control group. Oscillations occur around zero, then alternating correlated and anticorrelated behavior.

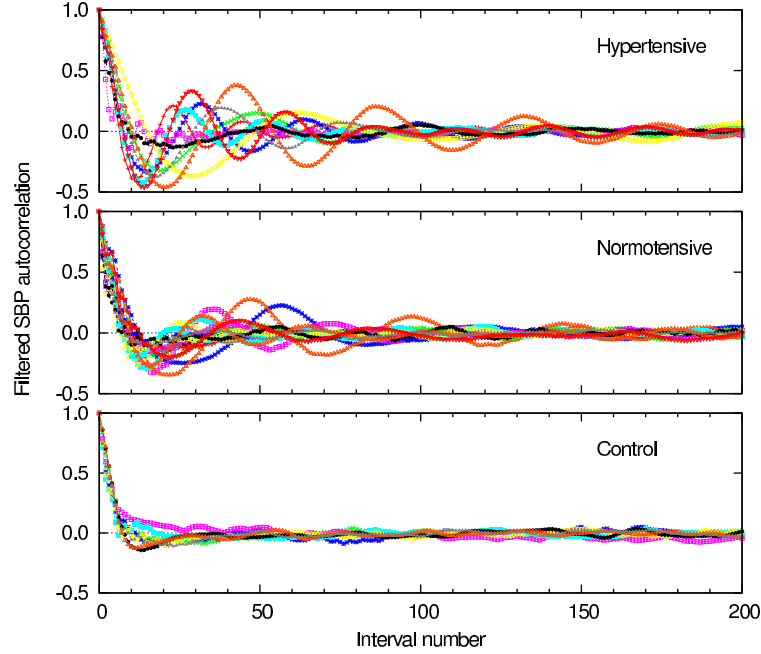


**Figure 8.** Autocorrelation of the filtered SBP time series, computed for all the individuals of each group.

Let us remark that according to the apnea score, the hypertensive subjects are in apnea during 28%, on average, of the records, while the normotensive ones are in apnea for 17%, on average. In this way, in general, the effects of apnea may be hidden, in particular in the case of correlations. Then, we look at the autocorrelation function for two fragments of the SBP time series: 2000 points during sleep apnea epochs and 2000 points in a non-apnea epoch, in order to compare the effects of apnea in the same patient. Fig. 9 shows the autocorrelation function for the original and filtered (local mean subtracted) signals. We clearly find this way that oscillations are related to apnea epochs. From the autocorrelation analysis, we conclude that the smaller amplitude of the oscillations in normotensive apneic subjects is not due to normal pressure but to a lower fraction of apnea epochs, then pointing to apnea as the source of the oscillations independently of the blood pressure condition.

In order to properly characterize the oscillations, we proceed to obtain the spectral density of the filtered signal, as illustrated in Fig. 10. It manifests a main peak localized at a frequency about 0.02 in units of inverse interval number. In fact, the peak is typically more pronounced in apneic subjects. Then, according to the discussion in the precedent paragraph, concerning the lower amplitude of the oscillations in normotensive subjects, we define a relative amplitude  $S^*$ , as the maximum value normalized by the integral of the spectrum in the interval  $[0.0, 0.1]$ . In Fig. 11, we represent the  $S^*$  against the apnea index, exhibiting the correlation between both quantities (with  $r = 0.74$ ).

Spectral analysis of interbeat interval increments has been previously carried out [19, 20]. In that case, the relative percentage of the very low frequency-component was taken as quantifier. However a ROC curve analysis presented a worse classification than in our case.

The ROC curves for the three quantities here considered as potential quantifiers, namely  $(S^*, \langle L \rangle, \langle \sigma^2 \rangle)$ , are

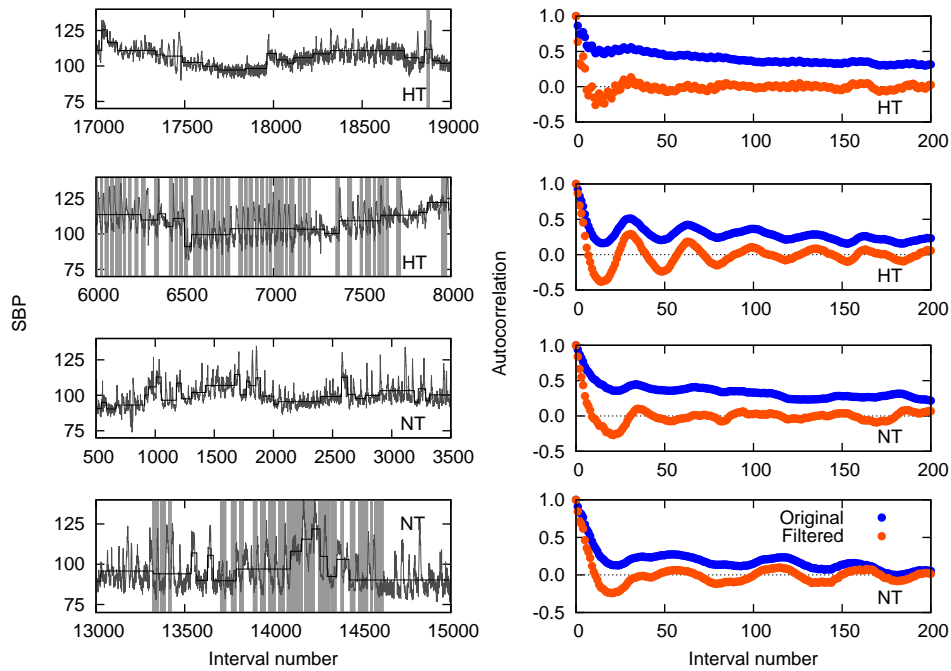


**Figure 9.** Left panels: Patches during non-apnea and apnea epochs (recognizable by the absence/presence of gray vertical lines), for hypertensive and normotensive subjects. Right panels: the corresponding autocorrelation function for the original and filtered (local mean subtracted) signals.

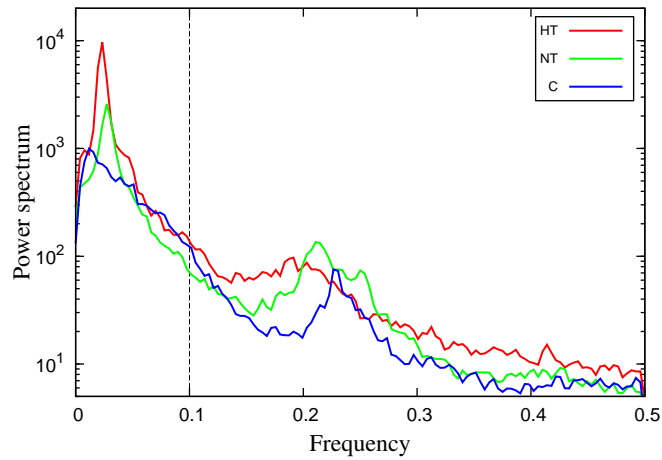


**Figure 10.** Power spectrum of the filtered SBP signal, for a typical individual of each group. Frequency corresponds to inverse interval number.

displayed in Fig. 12. From those curves, the respective thresholds were extracted. The accuracy (the sum of true positive and true negative subjects divided by the total sample size) of the optimal thresholds ( $S^*$ ,  $\langle L \rangle$ ,  $\langle \sigma^2 \rangle$ ) = (21.4, 112, 39) was 88, 82 and 82%, respectively.



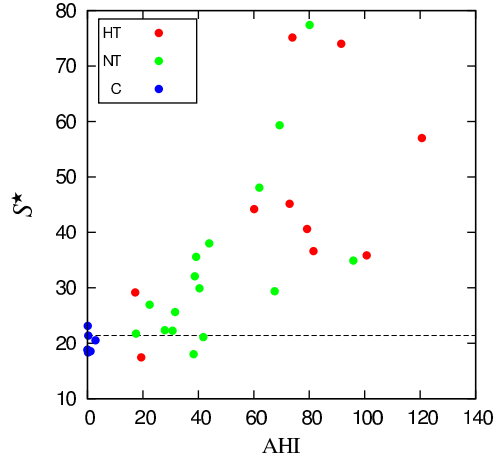


**Figure 11.** Normalized maximum  $S^*$  of the power spectrum versus AHI, for each individual. The dashed horizontal line represents the ROC threshold.

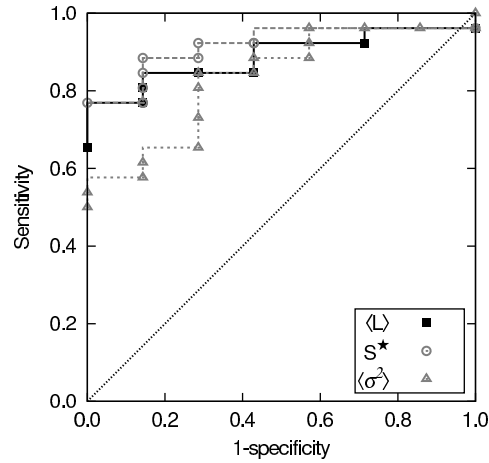


**Figure 12.** ROC curves for  $S^*$ ,  $\langle L \rangle$  and  $\langle \sigma^2 \rangle$ , obtained to identify patients with apnea. Threshold values (21.4, 112 and 39, respectively) shown in previous figures were obtained from the optimal classification corresponding to lowest distance to the upper left corner.

The two quantities displaying higher Pearson coefficient,  $r$ , with respect to the apnea index AHI are  $S^*$  and  $\langle L \rangle$ . Then we combine them to obtain the diagram shown in Fig. 13. We observe a neat separation of non-apneic subjects in the low  $S^*$  and low  $\langle L \rangle$  region.

## Discussion

We aim an alternative procedure for detecting apnea from simpler recordings than those composing a polysomnography. For that purpose, cardiovascular time series are good candidates. However, the nonstationarity of cardiovascular, as well as cardiorespiratory, data hampers to employ standard spectral techniques. Therefore, we apply a segmentation procedure, that has been recently developed [15], to identify the patches of stationary behavior.

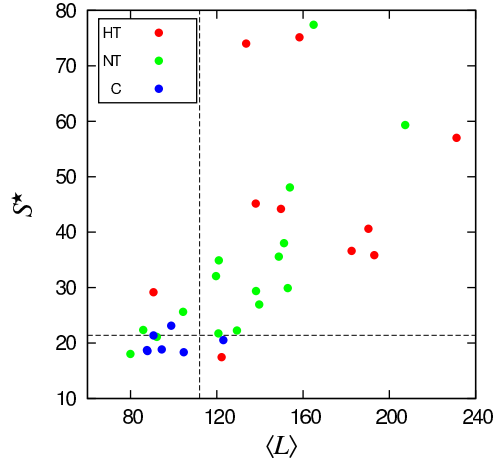


**Figure 13.** Normalized maximum of the spectral density  $S^*$  vs mean segment length  $\langle L \rangle$ , for each individual. Dashed lines represent threshold values.

Hence, for each patch, local quantities such as the statistical moments are well defined. Moreover, the filtered signal, where the local mean was subtracted furnishes a more stationary signal than the original one, hence it is more suitable, for instance, for spectral analysis.

Through segmentation, we detected features of the series that are correlated with apnea events. These features are the relative intensity  $S^*$  of the dominant oscillations in the autocorrelation function, the mean segment length  $\langle L \rangle$ , and, in a less extent, the average variance  $\langle \sigma^2 \rangle$ . According to the ROC curves, each of these quantities already shows a better performance than previous proposals based on heart rate increments [19,20]. Moreover, let us recall that obstructive sleep apnea was found to be better quantified using blood pressure variability, that are the data here considered, than heart rate increments [19]. The improvement may be attributed to our treatment of nonstationarity, which is absent in the abovementioned studies.

Furthermore, the healthy subjects had less larger patches than the patients (Fig. 2) which generally reflects a more active blood pressure regulation in a normal person. Hence, the combination of mean segment length and intensity of the oscillations allows to segregate apneic patients efficiently, as shown in Fig. 13. This furnishes an alternative procedure for the detection of apnea from SBP time series.

Let us also remark that a similar approach could be applied to other physiological issues, where nonstationarity is a common place.

## References

1. T. Penzel, N. Wessel, M. Riedl, J. W. Kantelhardt, S. Rostig, M. Glos, A. Suhrbier, H. Malberg, and I. Fietze, Cardiovascular and respiratory dynamics during normal and pathological sleep, *Chaos* **17**(1), 015116 (2007).
2. R. Stickgold, Sleep-dependent memory consolidation, *Nature* **437**, 1272 (2005).
3. C. Smith, Sleep states and memory processes, *Behav. Brain Res.* **69**, 137 (1995).
4. T. Penzel, J. McNames, P. de Chazal, B. Raymond, A. Murray, and G. Moody, Systematic comparison of different algorithms for apnoea detection based on electrocardiogram recordings, *MEDICAL & BIOLOGICAL ENGINEERING & COMPUTING* **40**(4), 402–407 (2002).

5. V. C. F. Helland, A. Gapelyuk, A. Suhrbier, M. Riedl, T. Penzel, J. Kurths, and N. Wessel, Investigation of an automatic sleep stage classification by means of multiscorer hypnogram, *Methods Inf. Med.* **49**, 467 (2010).
6. S. M. Caples, A. S. Gami, and V. K. Somers, Review Obstructive Sleep Apnea, **142**, 187–197 (2005).
7. H. M. Al-Angari and A. V. Sahakian, Use of Sample Entropy Approach to Study Heart Rate Variability in Obstructive Sleep Apnea Syndrom, *IEEE TRANSACTIONS ON BIOMEDICAL ENGINEERING* **54**, 1900 (2007).
8. T. Penzel, J. W. Kantelhardt, L. Grote, J.-H. Peter, and A. Bunde, Comparison of Detrended Fluctuation Analysis and Spectral Analysis for Heart Rate Variability in Sleep and Sleep Apnea, *IEEE TRANSACTIONS ON BIOMEDICAL ENGINEERING* **50**, 1143 (2003).
9. M. Mendez, D. Ruini, O. Villantieri, M. Matteucci, T. Penzel, S. Cerutti, and A. Bianchi, Detection of Sleep Apnea from surface ECG based on features extracted by an Autoregressive Model, in *Engineering in Medicine and Biology Society, 2007. EMBS 2007. 29th Annual International Conference of the IEEE*, pages 6105–6108, 2007.
10. A. Suhrbier, R. Heringer, T. Walther, H. Malberg, and N. Wessel, Comparison of three methods for beat-to-beat-interval extraction from continuous blood pressure and electrocardiogram with respect to heart rate variability analysis, *Biomed. Tech.* **51**, 70 (2006).
11. N. Wessel, H. Malberg, R. Bauernschmitt, and J. Kurths, Nonlinear methods of cardiovascular physics and their clinical applicability, *International Journal of Bifurcation and Chaos* **17**, 3325 (2007).
12. A. Gapelyuk, M. Riedl, A. Suhrbier, J. Krmer, G. Bretthauer, H. Malberg, J. Kurths, T. Penzel, and N. Wessel, Cardiovascular regulation in different sleep stages in the obstructive sleep apnea syndrome, *Biomed Tech (Berl)* **56**, 207 (2011).
13. A. Suhrbier, M. Riedl, H. Malberg, T. Penzel, G. Bretthauer, J. Kurths, and N. Wessel, Cardiovascular regulation during sleep quantified by symbolic coupling traces, *Chaos* **20**, 045124 (2010).
14. T. Penzel, M. Riedl, A. Gapelyuk, A. Suhrbier, G. Bretthauer, H. Malberg, C. Schöbel, I. Fietze, J. Heitmann, J. Kurths, and N. Wessel, Effect of CPAP therapy on daytime cardiovascular regulations in patients with obstructive sleep apnea, *Comput Biol Med.* **42**, 328 (2012).
15. S. Camargo, S. M. D. Queirós, and C. Anteneodo, Nonparametric segmentation of nonstationary time series, *Phys. Rev. E* **84**, 046702 (2011).
16. S. Camargo, M. Riedl, C. Anteneodo, N. Wessel, and J. Kurths, Diminished heart beat nonstationarities in congestive heart failure, *Frontiers in Physiology* **7**, 107 (2013).
17. T. Force, Guidelines - Heart rate variability, *European Heart Journal* **17**, 354 (1996).
18. C. E. Metz, Basic Principles of ROC Analysis, *Seminars in Nuclear Medicine* **VIII** (1978).
19. L. Poupard, I. Court-Fortune, V. Pichot, F. Chouchou, J.-C. Barthlmy, and F. Roche, Use of high-frequency peak in spectral analysis of heart rate increment to improve screening of obstructive sleep apnoea, *Sleep and Breathing* **15**, 837–843 (2011).
20. F. Roche, E. Sforza, D. Duverney, J.-R. Borderies, V. Pichot, O. Bigaignon, G. Ascher, and J.-C. Barthlmy, Heart rate increment: an electrocardiological approach for the early detection of obstructive sleep apnoea/hypopnoea syndrome, *Clin. Sci.* **107**, 105–110 (2004).